DALTON
FULL PAPER

Syntheses, structures and magnetic properties of two copper(II) diphosphonates: $[NH_3(CH_2)_2NH_3]_2[Cu_2(hedp)_2]\cdot H_2O$ and $[NH_3CH(CH_3)CH_2NH_3]_2[Cu_2(hedp)_2]$ (hedp = 1-hydroxyethylidenediphosphonate)

Hui-Hua Song,[a] Li-Min Zheng,*[a] Yong-Jiang Liu,[a] Xin-Quan Xin,[a] Allan J. Jacobson[b] and Silvio Decurtins[c]

[a] *State Key Laboratory of Coordination Chemistry, Coordination Chemistry Institute, Nanjing University, Nanjing 210093, P. R. China. E-mail: lmzheng@netra.nju.edu.cn*
[b] *Department of Chemistry, University of Houston, Houston, TX 77204, USA*
[c] *Department of Chemistry and Biochemistry, Bern University, Bern, Switzerland*

Received 13th March 2001, Accepted 13th September 2001
First published as an Advance Article on the web 17th October 2001

This paper describes the syntheses and characterization of two new copper(II) diphosphonates: $[NH_3(CH_2)_2NH_3]_2[Cu_2(hedp)_2]\cdot H_2O$ (**1**) and $[NH_3CH(CH_3)CH_2NH_3]_2[Cu_2(hedp)_2]$ (**2**) (hedp = 1-hydroxyethylidenediphosphonate). Both compounds exhibit similar one-dimensional linear chain structures. The symmetrical $\{Cu_2(hedp)_2\}$ dimers are connected by edge-shared $\{CuO_5\}$ square pyramids and form infinite chains. The Cu(II) ions are alternately bridged by O–P–O groups and O atoms. The Cu–O–Cu angles are 95.8(1) and 96.1(1)° for **1** and **2**, respectively. Their magnetic properties show moderately strong antiferromagnetic interactions in both compounds.

The metal phosphonates have been of increasing interest in recent years owing to their potential applications in exchange, catalysis and sensors.[1–9] Our efforts in exploring novel phosphonate materials with new structure types, based on 1-hydroxyethylidenediphosphonate [hedp, $CH_3C(OH)(PO_3)_2$], have been focused on studying template effects on the structures of transition metal–hedp compounds.[10] In a previous paper, we reported the syntheses and structures of a ladder-like chain compound $(NH_4)_2Cu_3(hedp)_2(H_2O)_4$ and two layer compounds $[NH_3(CH_2)_4NH_3][Cu_3(hedp)_2]\cdot 2H_2O$ and $[NH_2(C_2H_4)_2NH_2][Cu_3(hedp)_2]$,[11] where NH_3, 1,4-diaminobutane and piperazine were the templates. It has been found that the cations with larger sizes $\{[NH_3(CH_2)_4NH_3]^{2+}, [NH_2(C_2H_4)_2NH_2]^{2+}\}$ favor two-dimensional anionic layers, whereas the smaller cation (NH_4^+) directs the formation of an anionic chain.

By using ethylenediamine (en) and 1,2-propanediamine (1,2-pn) as templates, two new Cu–hedp compounds have been obtained which show novel chain structures. In this paper, the syntheses and crystal structures of these two compounds, namely $[NH_3(CH_2)_2NH_3]_2[Cu_2(hedp)_2]\cdot H_2O$ (**1**) and $[NH_3CH(CH_3)CH_2NH_3]_2[Cu_2(hedp)_2]$ (**2**), are described. Antiferromagnetic interactions are observed for both compounds.

Experimental

Materials and methods

All the starting materials were reagent grade used as purchased. The elemental analyses were performed with a PE 240C elemental analyzer. The infrared spectra were recorded on a IFS66V spectrometer with pressed KBr pellets. Thermal analyses were performed in nitrogen in the temperature range 30–600 °C with a heating rate of 5 °C min^{-1} on a TGA-DTA V1.1B TA Inst 2100 instrument. Variable-temperature magnetic susceptibility data were obtained on polycrystalline samples (14.62 mg for **1**, 31.82 mg for **2**) from 2 to 300 K in a magnetic field of 1 kG using a SQUID magnetometer. Diamagnetic corrections were estimated from Pascal's constants.[12] The temperature-independent paramagnetism (TIP) was estimated to be 60×10^{-6} cm^3 mol^{-1} for copper(II) mononuclear species.

Synthesis of $[NH_3(CH_2)_2NH_3]_2[Cu_2(hedp)_2]\cdot H_2O$, 1

A mixture of $Cu(NO_3)_2\cdot 3H_2O$ (1 mmol, 0.2490 g), a 50% aqueous solution of 1-hydroxyethylidenediphosphonic acid (50% $hedpH_4$) (2.5 mmol, 1 cm^3), LiF (1 mmol, 0.0258 g), $H_2C_2O_4\cdot 2H_2O$ (1 mmol, 0.1266 g) and H_2O (8 cm^3), adjusted by ethylenediamine to pH ≈ 4, was kept in a Teflon-lined autoclave at 140 °C for 3 d. After slow cooling to room temperature, blue needle-like crystals were collected as a monophasic material, judged by the powder X-ray diffraction pattern. Found (calcd.) for $C_8H_{30}Cu_2N_4O_{15}P_4$: C, 14.54 (14.27); H, 4.64 (4.49); N, 8.27 (8.32)%. IR (KBr, cm^{-1}): 3266m, 3043m (br), 1642m, 1550w, 1516w, 1479w, 1354w, 1089vs, 988m, 950m, 822w, 789w, 715w, 661m, 575s, 485w, 463w.

Synthesis of $[NH_3CH(CH_3)CH_2NH_3]_2[Cu_2(hedp)_2]$, 2

Hydrothermal treatment of a mixture of $Cu(NO_3)_2\cdot 3H_2O$ (1 mmol, 0.2418 g), 50% $hedpH_4$ (2.5 mmol, 1 cm^3), LiF (1 mmol, 0.0261 g) and H_2O (8 cm^3), adjusted by 1,2-propanediamine to pH ≈ 3, in a Teflon-lined autoclave at 140 °C for 2 d resulted in blue crystals of compound **2** as a single phase. Found (calcd.) for $C_{10}H_{32}Cu_2N_4O_{14}P_4$: C, 17.47 (17.57); H, 4.61 (4.72); N, 8.19 (8.20)%. IR (KBr, cm^{-1}): 3282m, 2940w, 1624m, 1550m, 1454m, 1356m, 1198m, 1093s, 1067vs, 990s, 947m, 922m, 818m, 685w, 663m, 572s, 487w, 463m.

Crystallographic studies

Single crystals of dimensions 0.20 × 0.24 × 0.24 mm for **1** and 0.60 × 0.20 × 0.20 mm for **2** were used for structure determinations. Compound **1** was measured on a Siemens SMART platform diffractometer equipped with a 1K CCD area detector using graphite-monochromated Mo-Kα (λ = 0.71073 Å) radiation. A hemisphere of data (1271 frames at 5 cm detector

DOI: 10.1039/b102346m

Table 1 Crystallographic data

Compound	**1**	**2**
Formula	$C_8H_{30}N_4Cu_2O_{15}P_4$	$C_{10}H_{32}N_4Cu_2O_{14}P_4$
M	673.32	683.36
T/K	223	293
Crystal system	Monoclinic	Monoclinic
Space group	$P2_1/n$	$C2/c$
a/Å	12.2579(10)	22.410(5)
b/Å	5.5010(4)	5.451(1)
c/Å	16.8746(13)	18.890(3)
β/°	101.1880(10)	107.13(2)
V/Å^3	1116.2(2)	2205.0(7)
Z	2	4
D_c/g cm^{-3}	2.003	2.058
F(000)	688	1400
μ(Mo-Kα)/cm^{-1}	22.71	22.98
Goodness of fit on F^2	1.178	1.052
$R1$, $wR2$[a] [$I > 2\sigma(I)$]	0.0295, 0.0843	0.0276, 0.0709
(all data)	0.0304, 0.0849	0.0388, 0.0752
Extinction coefficient/mm^{-1}	0.0073(7)	0.00033(14)
$(\Delta\rho)_{max}$, $(\Delta\rho)_{min}$/e Å^{-3}	0.769, −0.277	0.586, −0.728

[a] $R_1 = \Sigma||F_o| - |F_c||/\Sigma|F_o|$. $wR_2 = [\Sigma w(F_o^2 - F_c^2)^2/\Sigma w(F_o^2)^2]^{1/2}$.

distance) was collected using a narrow-frame method with scan widths of 0.30° in ω and an exposure time of 25 s per frame. The first 50 frames were re-measured at the end of data collection to monitor instrument and crystal stability, and the maximum correction applied on the intensities was <1%. The data were integrated using the Siemens SAINT program,[13] with the intensities corrected for Lorentz factor, polarization, air absorption, and absorption due to variation in the path length through the detector faceplate. The measurement of **2** was carried out on a Siemens P4 four-circle diffractometer with monochromated Mo-Kα (λ = 0.71073 Å) radiation. Cell constants and an orientation matrix for data collection were obtained from least-squares refinement of the setting angles of 43 randomly oriented reflections in the range 4.69 < θ < 9.02, corresponding to a monoclinic cell. As a check on crystal and instrument stability, three representative reflections were measured every 100, and a decay of 3.7% was observed for **2**. Intensity data were collected using the θ–2θ scan mode with a variable scan speed 5.0–50.0° min^{-1} in ω. The data were corrected for Lorentz-polarization effects during data reduction using XSCANS.[14] Number of measured and unique reflections: 5008, 1781 (R_{int} = 0.0248) for **1**; 4750, 1935 (R_{int} = 0.056) for **2**. Empirical absorption and extinction corrections were applied for both compounds.

The structures were solved by direct methods and refined on F^2 by full-matrix least squares using SHELXTL.[15] All the non-hydrogen atoms in both compounds were refined anisotropically except one C and one N atom of the $[NH_3(CH_2)_2NH_3]^{2+}$ cation in **1**. These two atoms are disordered over two sites, both at general positions with occupancy factors fixed at 0.75 [for C(4) and N(2)] and 0.25 [for C(4′) and N(2′)], respectively. The C–C and C–N constraints were used in further refinements. The $[NH_3CH(CH_3)CH_2NH_3]^{2+}$ cation in **2** is not disordered. The disordered C and N atoms in **1** and all hydrogen atoms were refined isotropically. The H atoms attached to C(4) [C(4′)] and N(2) [N(2′)] in **1** were not located. Crystallographic and refinement details are listed in Table 1, and selected bond lengths and angles in Tables 2 and 3 for **1** and **2**, respectively.

CCDC reference numbers 162088 and 162089.

See http://www.rsc.org/suppdata/dt/b1/b102346m/ for crystallographic data in CIF or other electronic format.

Results and discussion

Syntheses and preliminary characterization

Under hydrothermal conditions, compounds **1** and **2** have been prepared as single phases. As is well known, hydrothermal reactions usually involve a number of factors including the starting materials, the reaction temperature, pH, the reaction time and the presence of mineralizers which may significantly affect the crystallization of the final products. Such effects are observed in the synthesis of compound **1**. As described above, **1** was obtained by the hydrothermal reaction of a mixture of $Cu(NO_3)_2·3H_2O$, hedpH$_4$, en, LiF, $H_2C_2O_4·2H_2O$ and H_2O at 140 °C for 3 d. The molar ratio of Cu : hedp is 1 : 2.5. Both LiF and oxalic acid serve as mineralizers and help to crystallize the products. Compound **1** can be prepared in the absence of LiF and oxalic acid. The same compound was obtained at a higher reaction temperature (180 °C) or with an increased pH of the reaction mixture (pH ≈ 4–6). However, a similar reaction at a lower pH (≈ 3) led to the formation of a new phase based on the powder XRD pattern, which is formulated as $[NH_3(CH_2)_2NH_3][Cu_2(hedpH)_2]·2H_2O$ (**3**) according to elemental analysis.[16] This new phase also dominates when a higher molar ratio of Cu : hedp (2 : 2.5) is used while maintaining the pH at 3–4. Unfortunately, the crystal structure of compound **3** has not yet been solved because the crystals are multiply twinned.

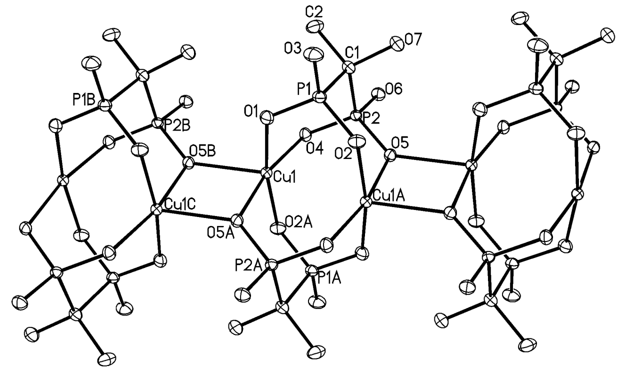

Fig. 1 A fragment of the $\{Cu_2(hedp)_2\}_n^{4n-}$ chain in structure **1** with the atomic labeling scheme (thermal ellipsoids shown at 50% probability).

The infrared spectra of **1** and **2** exhibit a series of bands in the 1000–1200 cm^{-1} range, corresponding to the phosphonate PO_3 group vibrations. Thermal analyses revealed that compound **1** loses weight in a single step decomposition below 220 °C. The weight loss is 3.4% (80–210 °C), slightly higher than that calculated (2.7%) for the removal of 1H$_2$O, possibly due to the partial decomposition of the organic components around 200 °C. No distinct weight loss is observed for **2** below 200 °C. Above 250 °C, the decomposition processes of **1** and **2** are similar and correspond to the release of protonated organic amines and the collapse of the polymeric structures. The final products were not identified in both cases. These thermal decomposition results are consistent with the single crystal structure determinations and elemental analyses.

Crystal structure of $[NH_3(CH_2)_2NH_3]_2[Cu_2(hedp)_2]·H_2O$, 1

Compound **1** crystallizes in space group $P2_1/n$. It has a linear chain structure with the diprotonated ethylenediamine cations located between the anionic $\{Cu_2(hedp)_2\}_n^{4n-}$ chains. Fig. 1 shows a fragment of the chain with atomic labeling scheme. The Cu atom has a square pyramidal geometry. The basal positions are occupied by O(1), O(4), O(2A) and O(5A) atoms from two equivalent hedp groups. The axial position is filled with O(5B) from a third hedp group. The mean deviation of the basal plane, defined by O(1), O(4), O(2A) and O(5A), is 0.0006 Å, with the largest deviation at the O(2A) atom (0.0007 Å). The Cu(1) atom lies 0.1926 Å above the basal plane. The Cu–O bond lengths [1.955(3)–2.224(3) Å] are comparable to those in $Na_2Cu_9(hedp)_6(OH)_2(H_2O)$[17] and other copper phosphonates,[11,18–22] though the axial Cu(1)–O(5B) distance [2.224(3) Å] is relatively longer (Table 2).

Table 2 Selected bond lengths [Å] and angles [°] for **1**

Cu(1)–O(1)	1.955(3)	Cu(1)–O(4)	1.968(3)
Cu(1)–O(2A)	1.972(3)	Cu(1)–O(5A)	1.995(2)
Cu(1)–O(5B)	2.224(3)	Cu(1)–Cu(1A)	2.9316(9)
P(1)–O(3)	1.513(3)	P(1)–O(2)	1.534(3)
P(1)–O(1)	1.536(3)	P(1)–C(1)	1.840(4)
P(2)–O(6)	1.520(3)	P(2)–O(4)	1.528(3)
P(2)–O(5)	1.543(3)	P(2)–C(1)	1.842(4)
O(1)–Cu(1)–O(4)	91.99(11)	O(1)–Cu(1)–O(2A)	168.70(12)
O(4)–Cu(1)–O(2A)	87.32(11)	O(1)–Cu(1)–O(5A)	89.24(11)
O(4)–Cu(1)–O(5A)	168.64(11)	O(2A)–Cu(1)–O(5A)	89.27(10)
O(1)–Cu(1)–O(5B)	95.84(10)	O(4)–Cu(1)–O(5B)	106.88(10)
O(2A)–Cu(1)–O(5B)	95.15(10)	O(5A)–Cu(1)–O(5B)	84.21(10)
Cu(1A)–O(5)–Cu(1C)	95.79(10)	P(1)–O(1)–Cu(1)	119.4(2)
P(1)–O(2)–Cu(1A)	121.8(2)	P(2)–O(4)–Cu(1)	121.8(2)
P(2)–O(5)–Cu(1A)	119.6(2)	P(2)–O(5)–Cu(1C)	138.2(2)

Symmetry transformations used to generate equivalent atoms: A, $-x + 2, -y + 1, -z + 1$; B, $x, y - 1, z$; C, $x, y + 1, z$.

Table 3 Selected bond lengths [Å] and angles [°] for **2**

Cu(1)–O(4)	1.9516(19)	Cu(1)–O(1)	1.964(2)
Cu(1)–O(5A)	1.9897(19)	Cu(1)–O(2A)	2.012(2)
Cu(1)–O(5B)	2.197(2)	Cu(1)–Cu(1A)	2.9076(8)
P(1)–O(3)	1.516(2)	P(1)–O(1)	1.529(2)
P(1)–O(2)	1.540(2)	P(1)–C(1)	1.835(3)
P(2)–O(6)	1.516(2)	P(2)–O(4)	1.532(2)
P(2)–O(5)	1.546(2)	P(2)–C(1)	1.843(3)
O(4)–Cu(1)–O(1)	91.23(9)	O(4)–Cu(1)–O(5A)	169.18(8)
O(1)–Cu(1)–O(5A)	87.67(8)	O(4)–Cu(1)–O(2A)	89.56(8)
O(1)–Cu(1)–O(2A)	168.88(8)	O(5A)–Cu(1)–O(2A)	89.48(8)
O(4)–Cu(1)–O(5B)	106.87(8)	O(1)–Cu(1)–O(5B)	96.14(8)
O(5A)–Cu(1)–O(5B)	83.95(8)	O(2A)–Cu(1)–O(5B)	94.25(8)
P(1)–O(2)–Cu(1A)	117.15(12)	P(2)–O(4)–Cu(1)	122.48(11)
P(2)–O(5)–Cu(1A)	119.79(12)	P(2)–O(5)–Cu(1C)	138.36(12)
Cu(1A)–O(5)–Cu(1C)	96.05(8)	P(1)–O(1)–Cu(1)	123.68(12)

Symmetry transformations used to generate equivalent atoms: A, $-x + 3/2, -y + 3/2, -z + 2$; B, $x, y + 1, z$; C, $x, y - 1, z$.

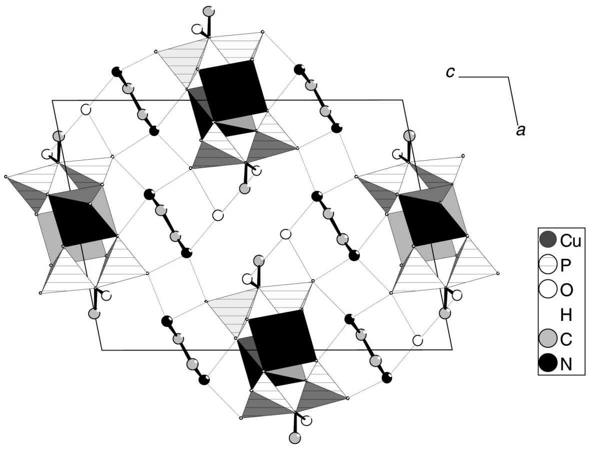

Fig. 2 Packing diagram of the structure of **1** along the [010] direction. $\{CuO_5\}$ square pyramidal (dark), $\{CPO_3\}$ tetrahedral (with horizontal line). The N(2′) and C(4′) are omitted for clarity.

Each hedp behaves as a bis(chelating) bridging ligand and links two copper ions in a *cis*-bridging mode, which is distinct from the *trans*-bridging mode observed in the other copper–hedp compounds.[10,11] The structure of the resulting $\{Cu_2(hedp)_2\}$ dimer is reminiscent of that of $Cu(OAc)_2{\cdot}H_2O$.[23] The Cu(1) · · · Cu(1A) distance [2.932 Å] in **1**, however, is significantly longer than that in $Cu(OAc)_2{\cdot}H_2O$ [2.65 Å] (Fig. 1). The atoms Cu(1) and Cu(1A) are related by an inversion center. The $\{Cu_2(hedp)_2\}$ dimers are connected by edge-shared $\{CuO_5\}$ square pyramids, forming infinite linear chains along the *b*-axis (Figs. 1 and 2). Thus, the Cu(II) ions are alternately bridged by O–P–O groups and O atoms. The Cu(1) · · · Cu(1C) distance within the oxygen bridged $\{Cu_2(\mu\text{-}O)_2\}$ dimers is 3.134 Å. The Cu(1)–O(5B)–Cu(1C) angle is 95.8(1)°. The protonated ethylenediamine and water molecules fill the spaces between the chains, and form an extensive hydrogen bonded network (Fig. 2). The three N(1) · · · O contacts are 2.732, 2.894 and 2.794 Å for N(1) · · · O(6)^{i}, N(1) · · · O(6)^{ii} and N(1) · · · O(2)^{iii} (symmetry code: i, $0.5 + x, 0.5 - y, 0.5 + z$; ii, $2 - x, 1 - y, 1 - z$; iii, $x, y - 1, z$), respectively. Hydrogen bonds may exist between the disordered nitrogen atom [N(2), N(2′)] and the phosphonate or water oxygens. The three N(2) · · · O contacts are 2.701, 2.728 and 2.781 Å for N(2) · · · O(3), N(2) · · · O(3)^{iv} and N(2) · · · O(1w)^{v} (symmetry code: iv, $1.5 - x, -0.5 + y, 1.5 - z$; v, $0.5 + x, 1.5 - y, 0.5 + z$), respectively.

Crystal structure of $[NH_3CH(CH_3)CH_2NH_3]_2[Cu_2(hedp)_2]$, 2

Compound **2** crystallizes in space group *C*2/*c*. The structure is closely related to that of **1**. It contains the same $\{Cu_2(hedp)_2\}^{4n-}_{n}$ chain with very similar bond distances and angles. The Cu(1) · · · Cu(1A) distance across the O–P–O bridge within the chain is 2.908 Å in **2** (Table 3). The Cu(1) · · · Cu(1C) distance across the O bridge and the Cu(1)–O(5B)–Cu(1C) angle are 3.115 Å and 96.1(1)°, respectively. An extensive hydrogen bonded network between the protonated amine and the chains is also found in **2** (Fig. 3). The N(1) · · · O(2), N(1) · · · O(6)^{i}, N(1) · · · O(6)^{ii} distances are 2.820, 2.827 and 2.708 Å (symmetry code: i, $1.5 - x, 0.5 - y, 2 - z$; ii, $x, 1 - y, 0.5 + z$), respectively. The N(2) · · · O(2), N(2) · · · O(3)^{iii} and N(2) · · · O(3)^{iv} distances are 3.092, 2.786 and 2.836 Å (symmetry code: iii, $1 - x, 1 - y, 2 - z$; iv, $x, y - 1, z$), respectively.

The structures **1** and **2** differ in the packing arrangements of the chains due to the different size and hydrogen bonding requirements of the cations that compensate the charges of the

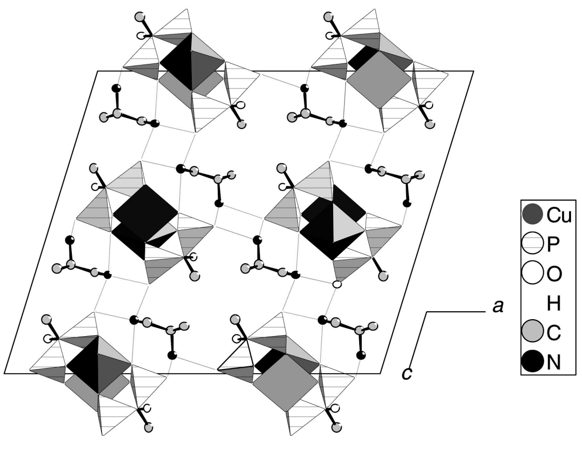

Fig. 3 Packing diagram of the structure of **2** along the [100] direction. $\{CuO_5\}$ square pyramidal (dark), $\{CPO_3\}$ tetrahedral (with horizontal line).

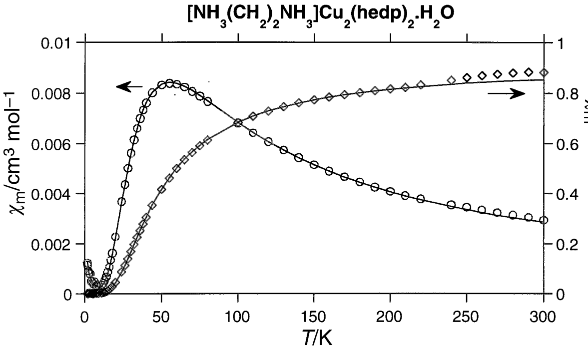

Fig. 4 χ_m and $\chi_m T$ *vs.* T plots for **1**. The solid line is the best fit to the Bleaney–Bowers expression.

anionic polymers. The protonated ethylenediamine in **1** and the protonated 1,2-propanediamine in **2** are different not only in size but also in their geometries and therefore in the directions of the hydrogen bonds. Compound **1** also includes a water molecule between the chains to further optimize the hydrogen bonding. Nevertheless, the fact that both cations direct the formation of chain structures in Cu–hedp compounds is consistent with previous observations.[11]

Magnetic properties

Fig. 4 shows the temperature dependent molar magnetic susceptibilities of **1** over the range 300–2 K. Upon cooling from room temperature, the χ_m value increases continuously until it reaches a maximum around 55 K, then decreases with decreasing temperature. Below 9 K, the χ_m value increases again. This magnetic behavior is characteristic of an antiferromagnetic interaction propagated between the magnetic centers together with a small amount of paramagnetic impurity.

As already described, compound **1** has a one-dimensional chain structure composed of $\{Cu_2(hedp)_2\}$ dimer units. Within the chain, the Cu(II) ions are bridged by O–P–O groups and oxygen atoms, alternately. The Cu···Cu distance through the O–P–O bridge is 2.932 Å, and that through the oxygen bridge is 3.134 Å (Fig. 1). The long Cu···Cu distances exclude an efficient direct exchange between the two copper(II) ions. Besides, the exchange coupling through the O–P–O bridge is expected to be weak because of the electron localization.[24] The observed antiferromagnetic interaction, therefore, should mainly arise from the magnetic superexchange through the oxygen bridges. The susceptibility data were analyzed by the Bleaney–Bowers expression for isotropic dimers of $S = 1/2$ ions based on the Heisenberg Hamiltonian $H = -JS_A \cdot S_B$.[12,25] The paramagnetic impurities manifested by the small upturns at low temperature were taken into account. An excellent fit, shown as a solid line in Fig. 4, is obtained with $g = 2.22$, $J = -61.8\ \mathrm{cm}^{-1}$, the molar fraction of noncoupled species (ρ) 0.00259. The coefficient of determination (r^2) is 0.99968.

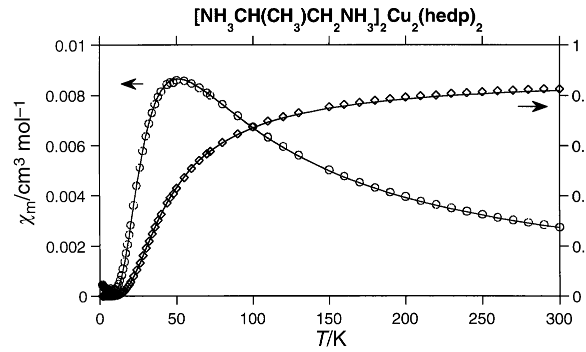

Fig. 5 χ_m and $\chi_m T$ *vs.* T plots for **2**. The solid line is the best fit to the Bleaney–Bowers expression.

Fig. 5 shows the χ_m and $\chi_m T$ *vs.* T plots for **2**. A maximum is again found in the χ_m *vs.* T curve around 50 K, indicating an antiferromagnetic interaction between the copper(II) ions. Since compound **2** has a similar chain structure to that of **1**, the magnetic behavior of **2** can be explained by exchange coupling within the $\{Cu_2(\mu\text{-}O)_2\}$ dimer. Theoretical fitting of the susceptibility data based on the isotropic dimer model leads to the parameters $g = 2.17$, $J = -57.3\ \mathrm{cm}^{-1}$, $\rho = 0.00118$ (Fig. 5). The coefficient of determination (r^2) is 0.99971.

Conclusion

Two new copper(II) diphosphonate compounds $[NH_3(CH_2)_2NH_3][Cu_2(hedp)_2]\cdot H_2O$ (**1**) and $[NH_3CH(CH_3)CH_2NH_3]_2[Cu_2(hedp)_2]$ (**2**) (hedp = $CH_3C(OH)(PO_3)_2$) have been synthesized under hydrothermal conditions. Although they crystallize in different space groups due to the different templates involved, their structures contain similar one-dimensional chains of $\{Cu_2(hedp)_2\}_n^{4n-}$. Within the chain, the symmetrical $\{Cu_2(hedp)_2\}$ dimers are connected by edge-shared $\{CuO_5\}$ square pyramids, with Cu–O–Cu angles of 95.8 and 96.1° for **1** and **2**, respectively. Antiferromagnetic interactions are found to be dominant for the two compounds.

Acknowledgements

Support from the National Natural Science Foundation of China (No. 29901003, 29823001) and the Analysis Center of Nanjing University are greatly acknowledged. The authors are indebted to Dr James D. Korp for crystallographic assistance in solving the structure of **1**, and to Adrian Schindler for magnetic measurements. This work made use of MRSEC/TCSUH Shared Experimental Facilities supported by the National Science Foundation under Award number DMR-9632667 and the Texas Center for Superconductivity at the University of Houston, USA.

References

1 G. Cao, H. Hong and T. E. Mallouk, *Acc. Chem. Res.*, 1992, **25**, 420.
2 G. Alberti, *Comprehensive Supramolecular Chemistry*, ed. J. M. Lehn, Pergamon, Elsevier Science, Ltd., Oxford, UK, 1996, vol. 7.
3 A. Clearfield, *Progress in Inorganic Chemistry*, ed. K. D. Karlin, John Wiley & Sons, Inc., New York, 1998, vol. 47, pp. 371–510.
4 G. Huan, J. W. Johnson, A. J. Jacobson and J. S. Merola, *J. Solid State Chem.*, 1990, **89**, 220.
5 J. L. Snover, H. Byrd, E. P. Suponeva, E. Vicenzi and M. E. Thompson, *Chem. Mater.*, 1996, **8**, 1490.

6 G. Alberti, U. Constantino, M. Casciola and R. Vivani, *Adv. Mater.*, 1996, **8**, 291.

7 K. Maeda, J. Akimoto, Y. Kiyozumi and F. Mizukami, *Angew. Chem., Int. Ed. Engl.*, 1995, **34**, 1199.

8 V. Soghomonian, Q. Chen, R. C. Haushalter and J. Zubieta, *Angew. Chem., Int. Ed. Engl.*, 1995, **34**, 223.

9 D. L. Lohse and S. C. Sevov, *Angew. Chem., Int. Ed. Engl.*, 1997, **36**, 1619.

10 L.-M. Zheng, H.-H. Song and X.-Q. Xin, *Comments Inorg. Chem.*, 2000, **22**, 129.

11 L.-M. Zheng, H.-H. Song, C.-Y. Duan and X.-Q. Xin, *Inorg. Chem.*, 1999, **38**, 5061.

12 O. Kahn, *Molecular Magnetism*, VCH Publishers, Inc., New York, 1993.

13 SAINT, Program for Data Extraction and Reduction, Siemens Analytical X-ray Instruments, Madison, WI, 1994–1996.

14 XSCANS (version 2.1), Siemens Analytical X-ray Instruments, Madison, WI, 1994.

15 SHELXTL (version 5.0), Reference Manual, Siemens Industrial Automation, Analytical Instrumentation, Madison, WI, 1995.

16 Elemental analysis: Found (calcd.) for $C_6H_{24}Cu_2N_2P_4O_{16}$: C, 11.81 (11.41); H, 3.83 (3.80); N, 4.46 (4.44)%.

17 L.-M. Zheng, C.-Y. Duan, X.-R. Ye, L.-Y. Zhang, C. Wang and X.-Q. Xin, *J. Chem. Soc., Dalton Trans.*, 1998, 905.

18 D. M. Poojary, B. Zhang and A. Clearfield, *J. Am. Chem. Soc.*, 1997, **119**, 12550.

19 D. M. Poojary, B. Zhang, P. Bellinghausen and A. Clearfield, *Inorg. Chem.*, 1996, **35**, 4942.

20 Y. Zhang and A. Clearfield, *Inorg. Chem.*, 1992, **31**, 2821.

21 J. Le Bideau, B. Bujoli, A. Jouanneaux, C. Payen, P. Palvadeau and J. Rouxel, *Inorg. Chem.*, 1993, **32**, 4617.

22 J. Le Bideau, C. Payen, P. Palvadeau and B. Bujoli, *Inorg. Chem.*, 1994, **33**, 4885.

23 A. F. Wells, *Structural Inorganic Chemistry*, Oxford University Press, New York, 1984.

24 H.-H. Song, L.-M. Zheng, C.-H. Lin, S.-L. Wang, X.-Q. Xin and S. Gao, *Chem. Mater.*, 1999, **11**, 2382.

25 B. Bleaney and K. D. Bowers, *Proc. R. Soc. London, Ser. A*, 1952, **214**, 451.